NANO LETTERS

pubs.acs.org/NanoLett Letter

DNA Knot Malleability in Single-Digit Nanopores

Rajesh Kumar Sharma, Ishita Agrawal, Liang Dai, Patrick Doyle,* and Slaven Garaj*

Cite This: https://dx.doi.org/10.1021/acs.nanolett.0c05142 Read Online

ACCESS | Metrics & More | Article Recommendations | Supporting Information

ABSTRACT: Knots in long DNA molecules are prevalent in biological systems and serve as a model system for investigating static and dynamic properties of biopolymers. We explore the dynamics of knots in double-stranded DNA in a new regime of nanometer-scale confinement, large forces, and short time scales, using solid-state nanopores. We show that DNA knots undergo isomorphic translocation through a nanopore, retaining their equilibrium morphology by swiftly compressing in a lateral direction to fit the constriction. We observe no evidence of knot tightening or jamming, even for single-digit nanopores. We explain the observations as the malleability of DNA, characterized by sharp buckling of the DNA in nanopores, driven by the transient disruption of base pairing. Our molecular dynamics simulations support the model. These results are relevant not only for the understanding of DNA packing and manipulation in living cells but also for the polymer physics of DNA and the development of nanopore-based sequencing technologies.

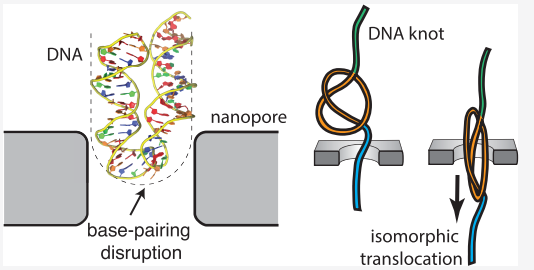

KEYWORDS: *Solid-state nanopores, DNA knots, polymers, DNA sequencing, knot dynamics*

Knots are a fundamental phenomenon in sufficiently long polymers.[1−4] Their presence in biomolecules such as DNA,[5−7] proteins,[8−14] and enzymes[15,16] and role in key processes like catalysis,[17] replication,[18,19] and DNA ejection from viral capsids[20−22] make them a crucial, yet scarcely understood, factor in biological processes in micro- and nanoconfinement. Previous reports have studied the knotting phenomena in spatially confined regions such as one-dimensional (1D) nanochannels and 2D nanoslits[23−25] but all in a quasi-static regime. Here, we explore the dynamics of the double-stranded DNA knots (ds-DNA) in a new regime of ultrahigh confinement, under large external forces, and at very short time scales, during the DNA translocation through nanopores. We found that DNA knots in this regime are highly malleable, capable of retaining their morphology during the translocation—showing no evidence of jamming and tightening—even for the nanopores whose diameter (5 nm) by far dwarfs the average theoretical equilibrium knot diameter ∼300 nm[26] and the DNA persistence length (∼50 nm). We show, using theoretical and computational modeling, that the malleability of knots is a unique feature of DNA polymers that stems from the localized melting in the highly constrained bends.

Nanopores are an indispensable tool for investigating the primary structure of biopolymers (DNA or protein sequence)[27,28] and polymer physics,[29] secondary structures in proteins,[30] and tertiary structures such as DNA knots.[31−33] An important question is—to what extent does the nanopore sensor itself alter the structure of the equilibrium DNA knots under investigation and how does the knot translocation dynamics depend on the dimensions of the nanopore constriction. Understanding the subject would allow us to confidently employ nanopores for high-throughput exploration of equilibrium properties of knotted polymers, including rare knotted structures that are otherwise inaccessible by the existing experimental techniques.[5,7,34−41]

In a typical experiment, a long DNA molecule is captured and electrophoretically translocated through a nanopore (Figure 1a). The translocating DNA blocks the pore, reducing the nanopore area available for ionic flow, and leads to a transient drop in the ionic current through the nanopore (Figure 1b). This current blockade $\Delta I_B(t)$ is a sensitive measure of the cross-sectional area of the part of the molecule that is passing through the pore at that moment.[42] The event charge deficit (*ecd*)[43] is defined as the total electrical charge prevented from passing through the nanopore due to the blocking molecule, $ecd = \int^{T_R} \Delta I_B(t)dt = \langle \Delta I_B \rangle \cdot T_R$, during the time of translocation T_R. The *ecd* should be conserved for freely translocating molecules, regardless of the DNA conformation during the process, as it scales with the volume of the molecule.

We observed the translocation of double-stranded (ds) lambda DNA molecules, 48.5 kilobase pair (kbp) long, at a bias voltage $V = 250$ mV. The measured DNA population is a mixture of circular and linear molecules, a portion of which are

Received: January 4, 2021
Revised: March 1, 2021

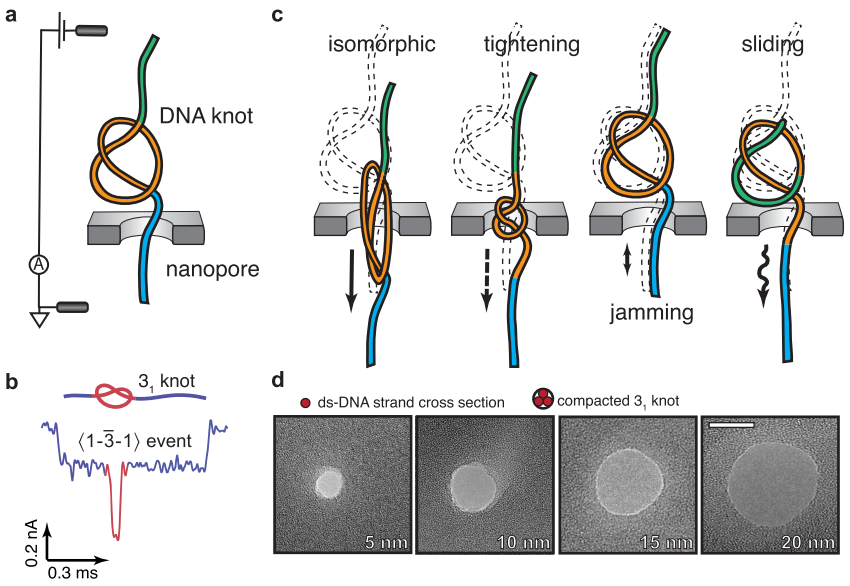

Figure 1. (a) Schematic of the translocation of a long knotted ds-DNA molecule through a nanopore in a free-standing silicon nitride (SiN_x) membrane. (b) As the knotted molecule passes through the nanopore, a transient resistive current blockage ΔI_B is observed, whose magnitude corresponds to the instantaneous number of strands translocating through the nanopore. The current−time trace of a molecule with a 3_1 knot shows that the current drop due to the knotted part is approximately three times that of the unknotted part of the molecule. The assigned digital signature ⟨1-3̄-1⟩ is based on the classification scheme described previously.[32] (c) Various scenarios in which a knotted molecule could translocate through a nanopore: isomorphic, tightening, jamming, and sliding. (d) Transmission electron microscope (TEM) images of the nanopores used in this work, with diameters of 5, 10, 15, and 20 nm. The scale bar is 10 nm. The upper inset shows the cross section of ds-DNA and the cross section of three compacted strands of a trefoil 3_1 knot, at the same scale as the TEM images.

knotted. The captured molecules experience a very strong force[44] of about 60 pN for a brief duration ($T_R \approx 0.8$ ms), which is much shorter than the Zimm relaxation time of ∼100 ms.[45,46] A simple DNA knot composed of three crossings, trefoil knot, experiences an even stronger force for duration of ∼10−100 μs.

When a DNA knot−significantly larger than the nanopore diameter−reaches the nanopore entrance, it could either undergo *isomorphic translocation* or it could get modified by several distortion mechanisms: *tightening*, *jamming*, *sliding*, or a combination of these (Figure 1c). For isomorphic translocation, the knot gets compressed longitudinally but retains all its prior information from the solution: contour length, crossings, position along the molecule, and topology.

A tightened knot would reduce in size compared to the equilibrium value due to the strong electric-field gradient pulling it on the two ends during translocation. A sliding event would occur if a knot hitting the mouth of the nanopore slides along the trailing edge of the DNA molecule to avoid entering the nanopore. Such a knot would either slide off from the linear DNA completely, and remain undetected, or slide for a period of time before eventually squeezing through the nanopore. A jamming event would occur if a knot reaching the nanopore entrance would lodge in, immobilizing DNA for a significant amount of time and noticeably increasing the overall translocation time.

As a knotted molecule traverses the nanopore, the transient drop in ionic current through the nanopore reveals the overall DNA and knot conformation.[32] Figure 1b shows the typical current drop signature of a molecule with a prime knot. The red-colored part of the signal indicates the combined current drop caused by the three strands of the 3_1 knot.

To understand the effect of nanopore constriction, we explore the dynamic knot distortions for a range of pore diameters D = 5, 10, 15, and 20 nm. The transmission electron microscope (TEM) images of the nanopores used in this study are shown in Figure 1d. The diameters of the pores obtained from TEM images are $D = (5.8 \pm 0.5)$ nm, $D = (10.5 \pm 0.5)$ nm, $D = (14.7 \pm 0.7)$ nm, and $D = (19.5 \pm 0.8)$ nm. The inset in Figure 1d shows the scaled cross section of ds-DNA and the cross section of three compacted strands of a trefoil 3_1 knot.[47] A previous study[48] concluded that the effective width of DNA inside the nanopore is $D_{DNA} = 2.1 \pm 0.2$ nm. Based on geometrical consideration, 5−7 strands of closely packed ds-DNA could be accommodated inside the $D = (5.8 \pm 0.5)$ nm pore, which accounts not only for simple prime knots but also for higher order prime knots and a variety of complex knots. Accordingly, we detected a maximum of 6 stranded knots inside the 5 nm pore and up to 14 stranded knots in the 20 nm pore (Figure S2).

KNOT TIGHTENING

Tightness of the knots in biomolecules affects their properties and functions.[49] If a knot has a propensity to tighten (i.e., reduce in size due to external forces) during its passage through a tight constriction, it would a) affect the dynamics of the biological threading processes and b) hinder the use of nanopores for investigating equilibrium properties of DNA knots in solution.

In Figure 2, we show the average contour length of the translocating knots $L_\varnothing$, as a function of the nanopore diameter. Previously, we have shown that a knot passing through a nanopore with diameter $D > 20$ nm does not exhibit any tightening−they have $L_\varnothing \approx 3$ μm and the corresponding equilibrium diameter $d_\varnothing \approx 300$ nm−and their size distribution follows closely the theoretical prediction for an unconfined polymer at equilibrium.[50] Our experiments cannot so far exclude the tightening of knots before they reach the

https://dx.doi.org/10.1021/acs.nanolett.0c05142
Nano Lett. XXXX, XXX, XXX−XXX

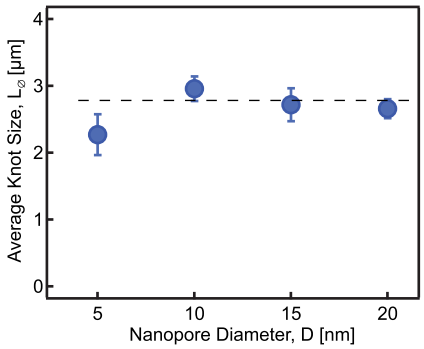

Figure 2. Average sizes of the knots in lambda DNA molecules as detected from nanopores of diameters D = 5−20 nm, measured in 1 M KCl aqueous salt solution, at a driving voltage V = 250 mV. The dashed line shows the average knot size for D = 10−20 nm pores.

nanopore—due to the tension propagation along the knotted DNA molecule[51] —but we believe it does not have a significant contribution to the currently used electrophoretic driving forces.

For all pores, we observe no significant, nanopore-induced tightening, with $L_{\varnothing}$ = 2.78 ± 0.16 μm for pores with diameters between D = 10−20 nm. A strong knot−nanopore interaction should lead to significant, progressive tightening as nanopores reduce in size, while we observe only a small reduction in the knot contour length using the smallest nanopore, $L_{\varnothing}$ (D = 5 nm) = 2.27 ± 0.31 μm. This slight effect might be explained by geometrical exclusion of higher-order knots in the small pore, not necessarily by the tightening. In contrast, another nanopore study[31] reported average knot contour length of about 0.7 μm for nanopore diameter D = 10 nm and other signs of knot distortions in the nanopores—it could be a consequence of the details of the interaction of pore walls and DNA (including the cleanliness of the pore) rather than an intrinsic effect.

Knot jamming refers to a scenario where a knot gets stuck at the nanopore entrance and halts the DNA translocation for a period of time. Jammed DNA might eventually translocate—maybe tightening the knot in the process—or it could diffuse back to the original chamber; but in both cases, the translocation time would significantly increase compared to the unimpeded translocation time for a DNA without a knot. Once the DNA threads the nanopore, the back-diffusion is an unlikely process due to large electrostatic energy of the DNA segment extended along the length of the nanopore channel.

To assess the jamming of knots, we plot in Figure 3a the ratio of the average event charge deficit for knotted (ecd_k) and unknotted (ecd_f) molecules, as a function of the nanopore diameter. If jammed, the knotted molecules should have noticeably increased translocation time and ecd_k. We do not observe any deviation of ecd_k from ecd_f, for all nanopore sizes, indicating that jamming is not relevant for any pore size.

Figure 3b shows the density map of the DNA translocation events in the D = 5 nm nanopore, plotted against the current blockade translocation time. Figure 3c shows the same plot for the subpopulation of knotted events. The knotted events follow a hyperbolic curve which represents *ecd* conservation, the same curve as the unknotted events (black line). Any spurious jamming would distort or offset the hyperbola due to the expected increase in the *ecd* of the jammed molecules.

Could jamming happen only for large knots, but the effect is obscured by much larger statistics of smaller knots? To test this hypothesis, we plot ecd_k versus knot size $L_{\varnothing}$ for all the knots measured in D = 5 nm and D = 20 nm nanopores (Figure 3d). Since we observe no variation in ecd_k with knot size, we

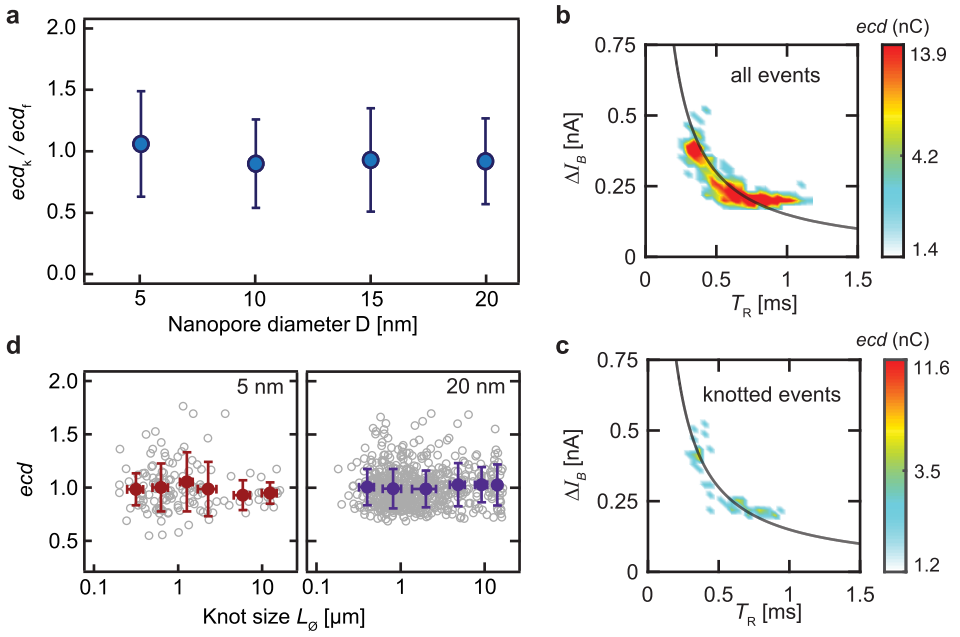

Figure 3. (a) Mean event charge deficit of knotted molecules (ecd_k) normalized by the mean event charge deficit of the unknotted molecules (ecd_k), as a function of the nanopore diameter. (b, c) Density map of average current blockade $\langle \Delta I_B \rangle$ vs the total translocation time T_R, for all events and for only knotted events, respectively (nanopore diameter D = 5 nm). The black hyperbola is the line of the constant *ecd*, the same in both cases. (d) Dependence of ecd_k for knotted events versus knot size $L_{\varnothing}$, presented for nanopores or D = 5 nm and D = 20 nm pores, shows an absence of any significant jamming of knots in both pores, regardless of the detected knot size. Gray open circles correspond to individual events, and filled circles correspond to average values in given intervals.

https://dx.doi.org/10.1021/acs.nanolett.0c05142
Nano Lett. XXXX, XXX, XXX−XXX

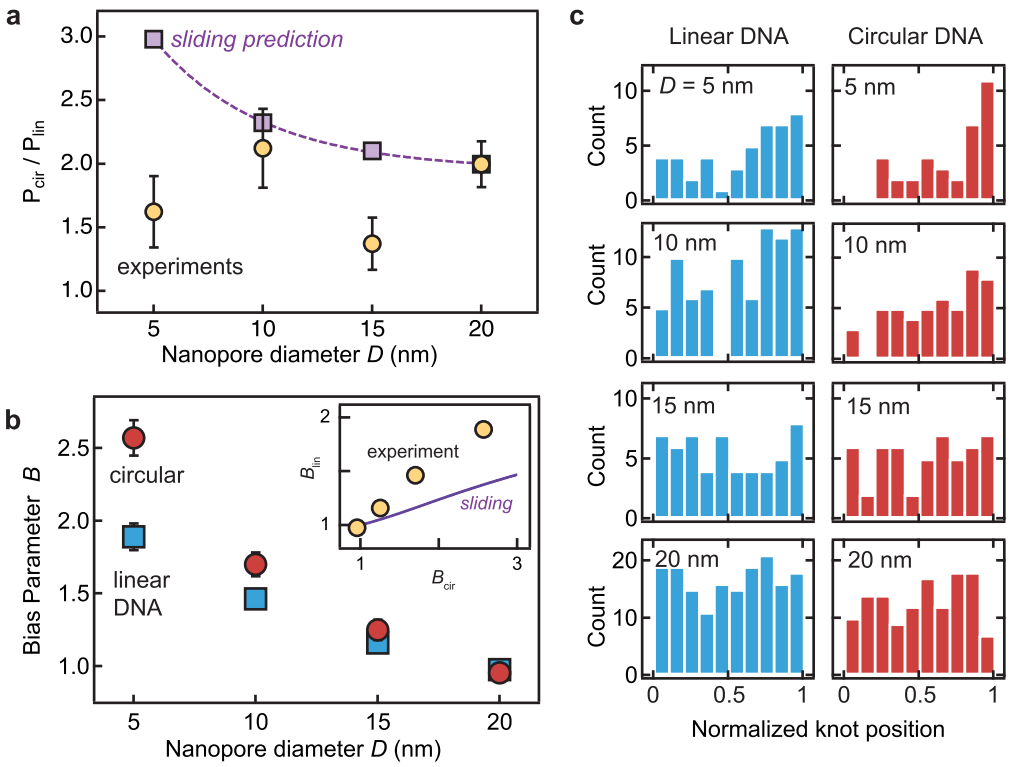

Figure 4. (a) Ratio of knotting probabilities in circular and linear lambda DNA molecules (P_{cir}/P_{lin}) with respect to the nanopore diameter. The experimental values (orange circles) do not follow predictions from the sliding model (purple squares), where increased sliding would lead to a decrease in detection of the knots in linear DNA. (b) Bias parameter B as a function of the nanopore diameter for linear (blue square) and circular (red circle) lambda DNA molecules. B measures the asymmetry in the knot distribution along the DNA molecule. The inset shows the relation between B parameters for circular and linear DNA, derived from the experiment (orange circles) and from the sliding model (purple line). (c) Histograms showing the positions of knots along the DNA molecules in 5−20 nm pores. Blue and red histograms correspond to the knot position in linear and circular lambda DNA molecules, respectively.

conclude that jamming does not play any significant role even for the D = 5 nm pore and larger knots, which is particularly interesting given that the nanopore diameter is much smaller than both the ds-DNA persistence length $L_p \approx 50$ nm and the average knot diameter in solution of ∼300 nm.

KNOT SLIDING

We investigate the potential effect of knot sliding by exploring knotting probability in circular and linear DNA and by examining the distributions of knot positions along the DNA.

In the case of knot sliding in linear DNA, some knots would completely slide off of the DNA molecule and would not be detected. The proportion of knotted $N_{knot}^{(lin)}$ vs all events $N_{total}^{(lin)}$ in the linear molecules $P_{lin} = N_{knot}^{(lin)}/N_{total}^{(lin)}$ should progressively decrease with the increasing sliding effect (i.e., for smaller nanopores). For circular molecules, the knots could not slide off due to the closed contour, and they should accumulate at the end of the DNA, not affecting the proportion of knotted molecules P_{cir}. We do not observe the trend of increasing $r_{cl} \equiv P_{cir}/P_{lin}$ with a decrease in the pore diameter (Figure 4a), revealing no noticeable slide-off effect.

Next, we look at the distribution of the knot positions along circular and linear molecules. We assume, if there is no sliding, that the position of signals from knots should be equally distributed along the current blockade curve $\Delta I_B(t)$ of the translocating DNA. If a knot slides along the DNA during translocation, it would be pushed toward the back end of the translocating molecule, shifting the weight of the distribution of the knot positions toward the end of the translocation event.

To quantify the phenomenon, we defined a *position-bias parameter* $B = 5 \cdot N_{20}/N_{tot}$ as the proportion of knots observed in the last 20% of the current blockade signal (N_{20}), over the total number of knots (N_{tot}).

Plotting B vs pore diameters (Figure 4b), we find a complete absence of position bias in large pores with diameter D = 20 nm, for both linear and circular DNA. As the diameter decreases, B increases. Histograms in Figure 4c−f show the normalized positions of knots in all the pores for both linear (blue) and circular (red) DNA. The progressive increase of B with the decreasing nanopore diameter could be attributed to two mechanisms: a) sliding of knots in the nanopores or b) dynamics of the DNA molecule during its capture in the solution.[52,53] Here, we explore both hypotheses.

To quantify the effect, we design a phenomenological knot-sliding model, which relies on a minimal set of assumptions that are robust against microscopic details of the sliding process, and nanopore−DNA interactions. We assume that knots have a given probability of sliding over a given distance that depends on the nanopore size, and we define it by the mean sliding length λ_S. The probability density for a knot sliding by distance Δx from its original position is derived as $\rho_s(\Delta x) = \lambda_S^{-1} \exp(\Delta x/\lambda_S)$. Sliding modifies the density distribution of knots along the linear molecules

$$c(x) = c_0\left(1 - \exp\left(-\frac{x}{\lambda_S}\right)\right) \quad (1)$$

https://dx.doi.org/10.1021/acs.nanolett.0c05142
Nano Lett. XXXX, XXX, XXX−XXX

where $c_0 = 1/L$ is the initial density of knots along the DNA of length L (we assume 1 knot per DNA). The knot density at positions $x > L$ represents the portion of knots that reach the end of the molecule—sliding off for the linear molecules and never detected or accumulating at the end for circular DNA. Using this distribution, we calculate bias parameters for circular and linear DNA $B_{cir}(\lambda_S,L)$ and $B_{lin}(\lambda_S,L)$, respectively, and the sliding loss of knots for linear molecules $\Delta P_{cir}(\lambda_S,L)$—see the Supporting Information for details. We derive $\lambda_S(D)$ from $B_{cir}(D)$ and use it to explore the relationship between the other observables and the consistency of the sliding assumption.

There are several inconsistencies between the sliding hypothesis and the observations. We do not observe a slide-off effect in Figure 4a, i.e., no decreasing trend in P_{cir}/P_{lin} for smaller pores, even while B_{cir} would indicate a large level of sliding with λ_S (5 nm) = 5.2 μm for the smallest pore. Next, B_{lin} has a much larger observed value than what is expected from B_{cir} (Figure 4b inset). Finally, with the accepted model of DNA translocation,[54−55] we would expect that a notable tightening accompanies significant knot sliding, such that the knot size reduction is related to the mean sliding length ($\Delta L_{\varnothing} \sim \lambda_S$)—none of which was observed.

There is an alternative hypothesis that could explain the observed trend for the B parameter. Past studies[52,56] have shown that a DNA random coil, trapped by the electric field gradient outside of the nanopore, spends significant time (milliseconds) probing the entrance of the nanopore before it is eventually translocated. In that scenario, a small pore could prefer an energetically favorable scenario where the DNA molecules, on average, enter the pore at a molecular position far from the knot, distorting the histogram of the knot positions and leading to an increased B parameter. This effect would depend on the number of strands participating in translocation and could lead to a difference in B_{lin} and B_{cir}.

MICROSCOPIC MECHANISM OF KNOT MALLEABILITY

To understand the malleability of DNA knots in single-digit nanopores—with the capacity to readily compact in the lateral direction without any significant tightening and jamming—we performed theoretical calculations and full-atom molecular dynamics simulations of DNA bending in nanopores. They reveal that the malleability is facilitated by the appearance of transient flexible hinges in the DNA polymer during large bending, defined by localized disruption of the base pairs. The hinges significantly lower the mechanical distortion energy for the polymer at nanometer-scaled loops, compared to the bending energy in the semiflexible chain model (Figure 5), allowing the electrophoretic force to induce folding.

We examine the passage of a folded double-stranded DNA section through the pore (*folded translocation*). The fold is the limiting part of the knot translocation process, where a knot has at minimum two folds and three strands to it. While entering a nanopore with diameter D = 5 nm, the DNA fold assumes a semicircular shape with the bending radius $R_c \approx (D-D_{DNA})/2 \approx 1.5$ nm (assuming dsDNA diameter $D_{DNA} \approx 2$ nm). The DNA bending energy in a wormlike chain model is $E_{bend} \approx (\pi L_p k_B T)/(2R_c) \approx 52.4 k_B T$.

A previous study,[57] calculating the cyclization of short ds-DNA molecules, suggested that a sharp bending can induce the disruption of the base pairing. The formation of such a flexible hinge requires a free energy of $E_{hinge} \approx 9-12 k_B T$, but it would

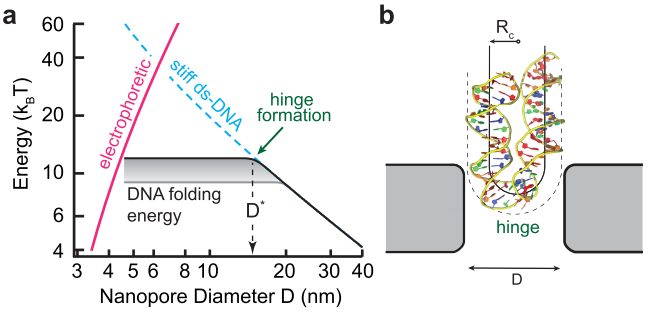

Figure 5. a) Energy diagram of the folding energy of ds-DNA and the work of the electrophoretic force acting on the DNA molecule folded in the nanopores (under applied voltage of 250 mV across the membrane). For larger nanopore diameters (D > 15 nm), the folding energy is dominated by the typical elastic bending, but for smaller nanopores (i.e., smaller DNA radius of curvature), it is determined by the energy of the hinge formation of locally melted base pairs. The shaded gray area represents the range of uncertainty. The blue dashed curve represents the expected folding energy if there would be no hinge formations. D^* is the limiting diameter below which the folding is dominated by hinge formation. The folding of the DNA molecules is expected in the regime where the electrophoretic work overcomes the folding energy. For smaller applied voltages, the hinge formation could be suppressed, leading to observable knot distortion. b) The DNA structure in the snapshot from our full-atom molecular dynamics simulation reveals formation of disrupted base pairs (hinge) in the translocating DNA loop.

substantially relieve the mechanical energy at the other DNA regions. Since $E_{hinge} \ll E_{bend}$ (D < 15 nm), hinge formation changes energy considerations for sharp DNA bends.

The knotted part of a DNA molecule experiences a very strong electrophoretic force[44] for a brief duration (~10−100 μs, much shorter than the Zimm relaxation time[5,45] of ~100 ms), so the folding force affects only the local segment of the knot at the nanopore entrance. The work of the electrophoretic force acting on the semicircular dsDNA segment in the nanopore (Figure 5b) is

$$P_e = \lambda_q l_{DNA} e\langle z\rangle = \lambda_q e(D - D_{DNA})^2 \quad (2)$$

The DNA contour length is $l_{DNA} \approx \pi R_c$; the average depth of the DNA half-circle in the nanopore is $\langle z\rangle \approx (2R_c)/\pi$; the linear charge density along the DNA is $\lambda_q \approx 5.9$ e/nm; e is the elementary charge; and the electric field strength in the nanopore is $\varepsilon = 1.67 \times 10^7$ V/m (assuming an applied voltage of 250 mV over a membrane thickness of L = 15 nm). Using the above values, we obtain $P_e \approx 17.1 k_B T$ for the smallest nanopore D = 5 nm, which is smaller than the bending energy but larger than the hinge formation energy, i.e., $E_{hinge} < P_e < E_{bend}$. As more DNA segments go deeper along the pore, the electric potential keeps increasing, but the bending energy saturates after forming a half-circle. The value $\Delta = (E_{hinge} - P_e)$ is the relevant energy barrier for the folded translocation, and it could be overcome in the D = 5 nm pore.

To confirm the malleability of DNA in a nanopore with diameter D = 5 nm, we performed full-atom molecular dynamics simulations (see the Methods section). It reveals the disruption of base pairing in the DNA molecule within the nanopore; a snapshot of the structure is given in Figure 5b. The DNA bending is localized at the region of the disrupted base pairs, which quickly restack once the bending force is relaxed. We conclude that the work performed by the driving electrophoretic force in the D = 5 nm nanopore is sufficient to

https://dx.doi.org/10.1021/acs.nanolett.0c05142
Nano Lett. XXXX, XXX, XXX−XXX

overcome DNA folding energy, chiefly due to local, transient disruption of the base pairs at the bend. The localized disruption of base pairs inside a nanopore prevents anchoring of a knot at the pore entrance—and the corresponding tightening, jamming, or sliding—leading to malleability of the knots in the few-nanometer regime. The base pair disruption needs to persist only for a short period of time <1 μs, while the fold threads the nanopore.

CONCLUSION

We explored, using nanopores, the dynamics of knotted DNA molecules in a new regime of nanometer-scale confinement, large forces, and short time scales. We showed that DNA knots, while translocating through nanopores, readily bend with the few-nanometer pore, swiftly compress in the lateral direction, and retain their equilibrium morphology. We explained the observed malleability of DNA polymers using a theoretical model and full-atom molecular dynamics simulations; we demonstrated that the translocating bends of the ds-DNA knots comprise a transient flexible hinge of melted base pairs that significantly lower the bending energy. The resulting isomorphic translocation of DNA knots, even in nanopores as small as 5 nm in diameter, validated nanopore microscopy as a relevant method for investigation of the equilibrium DNA knots. These results are relevant not only for the development of nanopore-based sequencing technologies but also for understanding DNA packing and dynamics in living cells. They offer insight into new polymer physics of malleable polymers that exhibit a breakdown of the fixed persistence length model in the high confinement regime.

METHODS

Nanopore Experiments. A nanopore chip consists of a silicon chip coated with a 300 nm thick low-stress silicon nitride SiN_X film, with a free-standing membrane in the center. A minimembrane, 500 nm in diameter, was further thinned down to 20 nm thickness, and the nanopore was drilled using a focused electron beam in a JEOL 2010F transmission electron microscope operating at 200 kV. DNA translocation experiments were performed in an aqueous salt solution, 1 M potassium chloride (KCl) buffered with 10 mM Tris and 1 mM ethylenediaminetetraaceticacid (EDTA), at pH = 8.2.

The double-stranded 48.5 kbp long lambda phage DNA sample was diluted to 5 μg/mL, heated to 65 °C for 5 min in 1 M KCl, and then rapidly cooled down on ice to form mixed populations of linear and circular DNA molecules.[58,59]

Nanopore conductivity measurements were performed using a pair of freshly regenerated Ag/AgCl electrodes connected to an Axopatch 200B amplifier with 250 mV driving voltage and a 50 kHz filter. All the experiments had a large statistical sample (1,000−4,500 events), and we have not observed any transient clogging of the nanopores. The knot length was determined as the contour size of the knot,[50] such that $L_{\varnothing} = L_{DNA} \cdot ecd_{knot}/ecd_{total}$. The velocity fluctuations during the translocation events are averaged out within the large statistics of the observed events.

More details are available in the Supporting Information.

Full Atom MD Simulations. We performed an all-atom molecular dynamics simulation of DNA translocation through a nanopore in the configuration shown in Figure 5, to examine whether the sharp bending induced by a nanopore can induce the disruption of DNA base pairs. We constructed a silicon nitride nanopore by deleting atoms within the pore region of a slab.[60] The atoms of the nanopore were frozen during the simulation. A straight DNA duplex of 41 base pairs was built using the 3DNA software system.[61] The canonical sequence was extracted from a prior experiment[62]

5′-GCGACTCTACGGAAGGGCATCCTTCGGGCATCACTACGCGC-3′

The system containing the nanopore and DNA molecule was solvated with TIP/3P water molecules and 1 M KCl. Initially, the DNA duplex was placed on top of the nanopore, parallel to the membrane. The large pulling of 360 pN was applied on the atoms to speed up the simulation. The all-atom MD simulation was performed using the GROMACS software package[63] with the OL15 force field[64] at the temperature of 300 K. Long-range electrostatics were treated using the particle mesh Ewald method, and a 1.0 nm cutoff was applied for van der Waals interactions and short electrostatic interactions. We run the simulation for time of 80 ns with a 2 fs step. We identified the disruption of 22nd, 23rd, and 24th base pairs by calculating distances between atoms involved in hydrogen bonds of base pairs.

ASSOCIATED CONTENT

Supporting Information

The Supporting Information is available free of charge at https://pubs.acs.org/doi/10.1021/acs.nanolett.0c05142.

Nanopore characterization, nanopore cleaning and assembly, nanopore characterization, DNA packing in nanopores, and analytical sliding model (PDF)

AUTHOR INFORMATION

Corresponding Authors

Patrick Doyle − *Singapore-MIT Alliance for Research and Technology Centre, Singapore 138602, Singapore; Department of Chemical Engineering, Massachusetts Institute of Technology, Cambridge, Massachusetts 02142, United States;* orcid.org/0000-0003-2147-9172; Email: pdoyle@mit.edu

Slaven Garaj − *Department of Physics, Centre for Advanced 2D Materials, and Department of Biomedical Engineering, National University of Singapore, Singapore 117542, Singapore;* orcid.org/0000-0001-5529-4040; Email: slaven@nus.edu.sg

Authors

Rajesh Kumar Sharma − *Department of Physics and Centre for Advanced 2D Materials, National University of Singapore, Singapore 117542, Singapore; Singapore-MIT Alliance for Research and Technology Centre, Singapore 138602, Singapore*

Ishita Agrawal − *Department of Biomedical Engineering, National University of Singapore, Singapore 117583, Singapore*

Liang Dai − *Department of Physics, City University of Hong Kong, Kowloon, Hong Kong, P. R. China;* orcid.org/0000-0002-4672-6283

Complete contact information is available at: https://pubs.acs.org/10.1021/acs.nanolett.0c05142

Author Contributions

S.G., P.S.D., and R.K.S. conceived the idea. R.K.S. and I.A. performed the experiments. R.K.S. analyzed the data. S.G.

https://dx.doi.org/10.1021/acs.nanolett.0c05142
Nano Lett. XXXX, XXX, XXX−XXX

developed the analytical sliding model. L.D. performed the simulations. All authors discussed the results and wrote the paper.

Notes

The authors declare no competing financial interest.

■ ACKNOWLEDGMENTS

This research is supported by the Agency for Science, Technology and Research (A*STAR) Singapore under its Advanced Manufacturing and Engineering (AME) Programmatic grant (Award A18A9b0060) and by the National Research Foundation, Prime Minister's Office, Singapore under its Campus for Research Excellence and Technological Enterprise (CREATE) program, through the Singapore MIT Alliance for Research and Technology (SMART): Critical Analytics for Manufacturing Personalised-Medicine (CAMP) Inter-Disciplinary Research Group.

■ REFERENCES

(1) Sumners, D. W.; Whittington, S. G. Knots in self-avoiding walks. *J. Phys. A: Math. Gen.* **1988**, *21*, 1689−1694.
(2) van Rensburg, E. J. J.; Sumners, D. A. W.; Wasserman, E.; Whittington, S. G. Entanglement complexity of self-avoiding walks. *J. Phys. A: Math. Gen.* **1992**, *25*, 6557−6566.
(3) Turner, J. C.; van de Griend, P. *History and science of knots*; World Scientific: 1996; DOI: 10.1142/2940.
(4) Meluzzi, D.; Smith, D. E.; Arya, G. Biophysics of knotting. *Annu. Rev. Biophys.* **2010**, *39*, 349−366.
(5) Bao, X. R.; Lee, H. J.; Quake, S. R. Behavior of complex knots in single DNA molecules. *Phys. Rev. Lett.* **2003**, *91*, 265506.
(6) Shaw, S. Y.; Wang, J. C. Knotting of a DNA chain during ring closure. *Science (Washington, DC, U. S.)* **1993**, *260*, 533−536.
(7) Rybenkov, V. V.; Cozzarelli, N. R.; Vologodskii, A. V. Probability of DNA knotting and the effective diameter of the DNA double helix. *Proc. Natl. Acad. Sci. U. S. A.* **1993**, *90*, 5307−5311.
(8) Taylor, W. R. A deeply knotted protein structure and how it might fold. *Nature* **2000**, *406*, 916−919.
(9) Ziegler, F.; et al. Knotting and unknotting of a protein in single molecule experiments. *Proc. Natl. Acad. Sci. U. S. A.* **2016**, *113*, 7533−7588.
(10) Jamroz, M.; et al. KnotProt: A database of proteins with knots and slipknots. *Nucleic Acids Res.* **2015**, *43*, D306−D314.
(11) Kolesov, G.; Virnau, P.; Kardar, M.; Mirny, L. A. Protein knot server: Detection of knots in protein structures. *Nucleic Acids Res.* **2007**, *35*, W425.
(12) Virnau, P.; Mirny, L. A.; Kardar, M. Intricate knots in proteins: Function and evolution. *PLoS Comput. Biol.* **2006**, *2*, 1074−1079.
(13) Taylor, W. R.; Lin, K. Protein knots: A tangled problem. *Nature* **2003**, *421*, 6918.
(14) Arai, Y.; et al. Tying a molecular knot with optical tweezers. *Nature* **1999**, *399*, 446−448.
(15) Nureki, O.; et al. An enzyme with a deep trefoil knot for the active-site architecture. *Acta Crystallogr., Sect. D: Biol. Crystallogr.* **2002**, *58*, 1129−1137.
(16) Nureki, O.; et al. Deep knot structure for construction of active site and cofactor binding site of tRNA modification enzyme. *Structure* **2004**, *12*, 593−602.
(17) Christian, T.; et al. Methyl transfer by substrate signaling from a knotted protein fold. *Nat. Struct. Mol. Biol.* **2016**, *23*, 941−948.
(18) Wang, J. C. Cellular roles of DNA topoisomerases: A molecular perspective. *Nat. Rev. Mol. Cell Biol.* **2002**, *3*, 430−440.
(19) Champoux, J. J. DNA Topoisomerases: Structure, Function, and Mechanism. *Annu. Rev. Biochem.* **2001**, *70*, 369−413.
(20) Matthews, R.; Louis, A. A.; Yeomans, J. M. Knot-controlled ejection of a polymer from a virus capsid. *Phys. Rev. Lett.* **2009**, *102*, 08101.
(21) Arsuaga, J.; et al. DNA knots reveal a chiral organization of DNA in phage capsids. *Proc. Natl. Acad. Sci. U. S. A.* **2005**, *102*, 9165−9169.
(22) Arsuaga, J.; Vázquez, M.; Trigueros, S.; Sumners, D. W.; Roca, J. Knotting probability of DNA molecules confined in restricted volumes: DNA knotting in phage capsids. *Proc. Natl. Acad. Sci. U. S. A.* **2002**, *99*, 5373−5377.
(23) Amin, S.; Khorshid, A.; Zeng, L.; Zimny, P.; Reisner, W. A nanofluidic knot factory based on compression of single DNA in nanochannels. *Nat. Commun.* **2018**, *9*, 1506.
(24) Dai, L.; Van Der Maarel, J. R. C.; Doyle, P. S. Effect of nanoslit confinement on the knotting probability of circular DNA. *ACS Macro Lett.* **2012**, *1*, 732−736.
(25) Orlandini, E.; Micheletti, C. Knotting of linear DNA in nanoslits and nano-channels: A numerical study. *J. Biol. Phys.* **2013**, *39*, 267−275.
(26) Dai, L.; Renner, C. B.; Doyle, P. S. Metastable tight knots in semiflexible chains. *Macromolecules* **2014**, *47*, 6135−6140.
(27) Branton, D.; et al. The potential and challenges of nanopore sequencing. *Nat. Biotechnol.* **2008**, *26*, 1146−1153.
(28) Timp, W.; Timp, G. Beyond mass spectrometry, the next step in proteomics. *Sci. Adv.* **2020**, *6*, No. eaax8978.
(29) Mihovilovic, M.; Hagerty, N.; Stein, D. Statistics of DNA capture by a solid-state nanopore. *Phys. Rev. Lett.* **2013**, *110*, 028102.
(30) Yusko, E. C.; et al. Real-time shape approximation and fingerprinting of single proteins using a nanopore. *Nat. Nanotechnol.* **2017**, *12*, 360−367.
(31) Plesa, C.; et al. Direct observation of DNA knots using a solid-state nanopore. *Nat. Nanotechnol.* **2016**, *11*, 1093−1097.
(32) Kumar Sharma, R.; Agrawal, I.; Dai, L.; Doyle, P. S.; Garaj, S. Complex DNA knots detected with a nanopore sensor. *Nat. Commun.* **2019**, *10*, 4473.
(33) Suma, A.; Micheletti, C. Pore translocation of knotted DNA rings. *Proc. Natl. Acad. Sci. U. S. A.* **2017**, *114*, E2991.
(34) Amin, S.; Khorshid, A.; Zeng, L.; Zimny, P.; Reisner, W. A nanofluidic knot factory based on compression of single DNA in nanochannels. *Nat. Commun.* **2018**, *9*, 1506.
(35) Klotz, A. R.; Narsimhan, V.; Soh, B. W.; Doyle, P. S. Dynamics of DNA Knots during Chain Relaxation. *Macromolecules* **2017**, *50*, 4074−4082.
(36) Tang, J.; Du, N.; Doyle, P. S. Compression and self-entanglement of single DNA molecules under uniform electric field. *Proc. Natl. Acad. Sci. U. S. A.* **2011**, *108*, 16153−16158.
(37) Krasnow, M. A.; et al. Determination of the absolute handedness of knots and catenanes of DNA. *Nature* **1983**, *304*, 559−560.
(38) Wiggins, P.; et al. High flexibility of dna on short length scales probed by atomic force microscopy. *Nat. Nanotechnol.* **2006**, *1*, 137−141.
(39) Hansma, H. G. Surface biology of DNA by atomic force microscopy. *Annu. Rev. Phys. Chem.* **2001**, *52*, 71−92.
(40) Trigueros, S. Novel display of knotted DNA molecules by two-dimensional gel electrophoresis. *Nucleic Acids Res.* **2001**, *29*, 67.
(41) Wasserman, S. A.; Cozzarelli, N. R. Biochemical topology: Applications to DNA recombination and replication. *Science (Washington, DC, U. S.)* **1986**, *232*, 951−960.
(42) Li, J.; et al. Ion-beam sculpting at nanometre length scales. *Nature* **2001**, *412*, 166−169.
(43) Fologea, D.; et al. Detecting single stranded DNA with a solid state nanopore. *Nano Lett.* **2005**, *5*, 1905−1909.
(44) Keyser, U. F. Direct force measurements on DNA in a solid-state nanopore. *Nat. Phys.* **2006**, *2*, 473.
(45) Liu, Y.; Jun, Y.; Steinberg, V. Longest relaxation times of double-stranded and single-stranded DNA. *Macromolecules* **2007**, *40*, 2172−2176.
(46) Klotz, A. R.; Soh, B. W.; Doyle, P. S. Motion of Knots in DNA Stretched by Elongational Fields. *Phys. Rev. Lett.* **2018**, *120*, 188003.
(47) Alexander, J. W.; Briggs, G. B. Annals of Mathematics On Types of Knotted Curves. *Second Ser.* **1926**, *28*, 562.

https://dx.doi.org/10.1021/acs.nanolett.0c05142
Nano Lett. XXXX, XXX, XXX−XXX

(48) Garaj, S.; Liu, S.; Golovchenko, J. A.; Branton, D. Molecule-hugging graphene nanopores. *Proc. Natl. Acad. Sci. U. S. A.* **2013**, *110*, 12192−12196.
(49) Zhang, L.; et al. Effects of knot tightness at the molecular level. *Proc. Natl. Acad. Sci. U. S. A.* **2019**, *116*, 2452−2457.
(50) Kumar Sharma, R.; Agrawal, I.; Dai, L.; Doyle, P. S.; Garaj, S. Complex DNA knots detected with a nanopore sensor. *Nat. Commun.* **2019**, *10*, 4473.
(51) Suma, A.; Micheletti, C. Pore translocation of knotted DNA rings. *Proc. Natl. Acad. Sci. U. S. A.* **2017**, *114*, E2991−E2997.
(52) Vlassarev, D. M.; Golovchenko, J. A. Trapping DNA near a solid-state nanopore. *Biophys. J.* **2012**, *103*, 352−356.
(53) Kowalczyk, S. W.; Dekker, C. Measurement of the docking time of a DNA molecule onto a solid-state nanopore. *Nano Lett.* **2012**, *12*, 4159−4163.
(54) Lu, B.; Albertorio, F.; Hoogerheide, D. P.; Golovchenko, J. A. Origins and consequences of velocity fluctuations during DNA passage through a nanopore. *Biophys. J.* **2011**, *101*, 70−79.
(55) Plesa, C.; Van Loo, N.; Ketterer, P.; Dietz, H.; Dekker, C. Velocity of DNA during translocation through a solid-state nanopore. *Nano Lett.* **2015**, *15*, 732−737.
(56) Kowalczyk, S. W.; Dekker, C. Measurement of the docking time of a DNA molecule onto a solid-state nanopore. *Nano Lett.* **2012**, *12*, 4159−4163.
(57) Yan, J.; Marko, J. F. Localized single-stranded bubble mechanism for cyclization of short double helix DNA. *Phys. Rev. Lett.* **2004**, *93*, 108108.
(58) Wang, J. C.; Davidson, N. Thermodynamic and kinetic studies on the interconversion between the linear and circular forms of phage lambda DNA. *J. Mol. Biol.* **1966**, *15*, 111−123.
(59) Plesa, C.; et al. Direct observation of DNA knots using a solid-state nanopore. *Nat. Nanotechnol.* **2016**, *11*, 1093.
(60) Aksimentiev, A.; Heng, J. B.; Timp, G.; Schulten, K. Microscopic kinetics of DNA translocation through synthetic nanopores. *Biophys. J.* **2004**, *87*, 2086−2097.
(61) Lu, X. J.; Olson, W. K. 3DNA: A software package for the analysis, rebuilding and visualization of three-dimensional nucleic acid structures. *Nucleic Acids Res.* **2003**, *31*, 5108−5121.
(62) Mathew-Fenn, R. S.; Das, R.; Harbury, P. A. B. Remeasuring the double helix. *Science (Washington, DC, U. S.)* **2008**, *322*, 446−449.
(63) Abraham, M. J.; et al. Gromacs: High performance molecular simulations through multi-level parallelism from laptops to supercomputers. *SoftwareX* **2015**, *1*, 19−25.
(64) Zgarbová, M.; et al. Refinement of the Sugar-Phosphate Backbone Torsion Beta for AMBER Force Fields Improves the Description of Z- and B-DNA. *J. Chem. Theory Comput.* **2015**, *11*, 5723−5736.

https://dx.doi.org/10.1021/acs.nanolett.0c05142
Nano Lett. XXXX, XXX, XXX−XXX